行政院國家科學委員會專題研究計畫　期中進度報告

小型熱聲冷凍機製造及研究 (1/3)

計畫類別： 個別型計畫
計畫編號： NSC91-2212-E-002-098-
執行期間： 91 年 08 月 01 日至 92 年 07 月 31 日
執行單位： 國立臺灣大學應用力學研究所

計畫主持人： 胡文聰

報告類型： 精簡報告
報告附件： 出席國際會議研究心得報告及發表論文
處理方式： 本計畫可公開查詢

中　華　民　國 92 年 5 月 30 日

行政院國家科學委員會專題研究計畫成果報告

小型熱聲冷凍機製造及研究 (1/3)

計畫執行起訖: 2002.08.01 至 2003.07.31

計畫編號 91-2212-E-002-098

國立台灣大學應用力學研究所

主持人: 胡文聰

中文摘要

本計劃欲分三年執行，總目的為設計、製造及分析一小型熱聲學冷凍機。“小型”指冷凍機之特徵長度為公分尺度(第一年)到公釐(第二年)，但將使用 MEMS 製程製造關鍵零件在各年中。第一年將進行系統設計、使用矽製造 stack 關鍵零件、安裝在熱聲冷凍機平台中、及測試。第二年將專注於熱聲 driver 之設計、製造及測試。第三年將進行熱聲冷凍機系統整合、製造及測試。

第一年目標在熱聲機中關鍵零件: stack。計劃中將使用矽製造數件 MEMS stack 片，並將 stack 片疊整齊，stack 片與 stack 片間使用低熱傳導材料隔離。MEMS stack 片之物理動機在於降低聲波軸向之熱傳導(以空氣為主，熱傳導係數約 0.025W/m-K)並增加聲波徑向之熱傳導(以矽為主，熱傳導係數約 150W/m-K)。Stack 片疊將安裝在一活塞為 driver (最大 300Hz.)之共振器中。矽 stack 量測結果將與陶瓷 stack 比較。數值計算及設計將使用熱聲學程式 DeltaE。

Abstract

This three-year proposal aims at design, fabrication and experimental study of small cooling devices. The term ‘small cooling devices’ implies cooling systems whose overall length-scale ranges from centimeter (first year focus) to millimeter (second year focus), but with MEMS fabricated components throughout the course of the three-year project (as an example, see Fig. 8). The first year will focus on the *stack*, perhaps the key component in a thermoacoustic device, and its performance. The second year will focus on the *driver* (micro-speaker) and its performance. The focus of the third year would be to integrate results from the first two years.

The *first year focus* is on the design and testing of a new small-scale thermoacoustics refrigerator *stack* using micro-machined technique. The unique approach is to use several MEMS fabricated silicon wafers with equally spaced gap as the stack. The motivation is based on the physic of suppressing conduction heat transfer (due to the air gap) in the direction of acoustic oscillation while encouraging heat transfer in the normal direction, since thermal conductivity of silicon (150W/m-K) is much higher than that of air (0.025W/m-K). The stack assembly will be mounted adjacent to an oscillating piston (max 300 Hz) as an acoustic source. Results will be compared with a ceramic stack as baseline as well as computation by a linear acoustic code DeltaE.

Introduction

Ongoing research and application of the thermoacoustic effect to engines and refrigerators has demonstrated the usefulness of the thermoacoustic effect for practical applications. Many groups are currently investigating the potential for smaller physical scale operation. The target application is in electronic cooling where the trend is toward higher power dissipation in smaller packages leading to ever-increasing cooling demands. Present passive cooling methods using thermal heat spreaders, including heat pipes, and convective air cooling are reaching their limits. For this reason, researchers are looking at ways of lowering the sink temperature as well as increasing heat transfer coefficients. A thermoacoustic heat pump provides one

potential method for active cooling.

The physical challenges of reducing the scale of a heat engine or heat pump are worthy of consideration. From a thermodynamic point of view, any heat engine will be more efficient when operating at larger temperature differences. However, as engine size is reduced, efficiency cannot be maintained due to the increasing proportion of parasitic (perimeter) heat loss. Therefore, at some small scale a heat engine is no longer practical. However, a heat pump, which operates at a relatively lower temperature difference, may be efficient enough at sufficiently small scale to be useful in an electronics cooling application.

The current effort attempts to take a step toward miniaturization by testing heat-pump stack designs that are more amenable to micro-scale cooling applications. This work presents the design of a new small-scale thermoacoustics test platform (mTAP), Fig. 1, which is a variable length (maximum 10 cm) and frequency, fixed piston stroke, below-resonance device. In addition, the performance of a discontinuous "Si spaced-wafer stack" is presented along with comparable data from a ceramic rectangular-pore stack, and numerical modeling.

The goal of the current research is to determine the best performance of this Si wafer stack with the testing and numerical modeling of the ceramic stack providing a baseline for comparison. Previous work in the Microscale Thermofluids lab at NTU used the same ceramic stack material at a larger scale in a thermoacoustic engine driven thermoacoustic refrigerator (Holmberg *et. al*., 2001).

The Si spaced-wafer stack (SiSWS) and mTAP design are presented next followed by experimental stack performance and comparison to numerical data.

Si SPACED-WAFER STACK

The SiSWS stack is effectively a stack of Si wafers with low thermal conductivity spacer rings inserted between the Si wafers, Fig. 2. Each wafer is etched with a parallel plate (PP) structure, resembling a 0.5mm long slice from a PP stack made of silicon, Fig. 3. The Si filaments ("plates") themselves are 0.2mm wide and 0.5mm long (wafer thickness) in the flow direction, with 1.1 mm spacing between filaments. The wafers are separated from each other by the spacer rings which are varied in thickness for testing purposes.

Using a stack formed from Si wafers has multiple potential benefits. First, using silicon processing techniques may allow for cheaper stacks with smaller feature sizes. Easier fabrication and integration into a cooling system are also hoped for. Beyond this, the Si wafer stack approach has the potential for increased efficiency. This benefit stems primarily from the broken heat transfer path across the stack (not a continuous solid), as well as from low volume porosity.

Research with other non-standard stacks lends support to the potential benefits of the Si-wafer stack. The work of Adeff et. al. (1998) looked at the performance of reticulated vitreous carbon (RVC—open cell foam with 97% volume porosity) stacks. RVC stacks of different cell pore size were tested in place of existing plastic roll stacks in two devices, acting as a prime mover stack in the first device and as heat pump in the second. Results indicate that the RVC stack performed in most cases better than the PP stacks over the tested ranges. The optimum pore size for the RVC stacks (in pores per inch) was shown to be approximately equal to that for the PP stacks (plates per inch), although larger pore RVC stacks performed at higher efficiency. Further analysis of the data in the paper shows that the RVC stacks perform at higher efficiency than the PP stacks for lower power levels, but that the PP stacks perform better when power demand (prime mover) or load (heat pump) are above a certain level. For their experiments, higher power corresponds to higher pressure fluctuation levels, and thus higher fluid Reynolds numbers in the stacks. It is expected, given the RVC structure of carbon filaments oriented in all directions, that the RVC will have viscous losses increasing non-linearly with Re, whereas this will not be the case with a smooth PP stack. This might explain the poorer performance of the RVC at higher power levels. On the other hand, the RVC stack's open structure has a higher volume

porosity with lower solid thermal conduction along the stack, so higher efficiency at lower power levels might be expected. However, no thermal/ viscous modeling of this complex structure has been performed to confirm these ideas.

Bosel *et. al.* (1999) modeled and tested an "interrupted stack" (IS) design which has parallel plate goemetry but with 2 mm stack segments (in the flow direction) with alternating 90° orientation and only very thin spacer rings. They did see better performance numerically and experimentally from the IS stack than the continuous parallel plate stack. The IS stack saw performance increases of up to 50% at the highest power load settings. Optimum plate spacing was found to be equal to that for the continuous stack. Although measured work input (viscous losses) were slightly higher, COP values for the IS were still significantly higher.

By comparison, the SiSWS used here has a high volume porosity similar to the RVC, and thus can put more gas parcels to work. It has no physical solid connection along the length (except at the perimeter spacers), and therefore will have very low solid thermal conduction along the stack. Compared to a pin stack, which has all filaments oriented with the flow, the Si wafer stack has no filament oriented with the flow, but rather across the flow, and these filaments can be expected to suffer from drag problems at higher Re. Compared to the IS, the PP sections have been reduced to a minimum length, while the air gap between wafers (spacer thickness) has been increased. In addition, for these tests, Si wafers are stacked with all filaments oriented in the same direction, which may reduce viscous losses at higher Re due to downstream filaments operating in the wake of upstream filaments.

The actual scaling of filament spacing and inter-wafer air gap can be seen in Fig. 4. Any air packet oscillating within this stack must be able to transfer heat with some solid (filament) surface at the end of its displacement stroke. Therefore, just as the optimal spacing between filaments (PP stack design, e.g., as discussed in Swift, 2000) should be approximately 4 or 5 thermal penetration depths (δ_k), this same rule of thumb should apply to the inter-wafer separation distance. This is one hypothesis of this research.

DEVICE DESIGN

The mTAP device itself (Fig. 1) was initially conceived as a piezo-actuator driven, ¼ wavelength 3 kHz resonator. This was abandoned due to the uncertainty of generating sufficient power with the piezo, as well as the very small scale of stack pores required for efficient operation using one atmosphere air as the driving gas. Presently, a modified radio controlled airplane piston engine is driven in reverse by a variable speed motor that moves the piston at speeds up to 300Hz. The piston allows for a known uniform velocity profile (and thus known work input) and also has power to move air with a significant fluctuation amplitude. The device operates below resonance, which allows for independent variation of thermal penetration depth as well as larger pore sizes in the stack.

The piston and stack internal diameters are 20 mm. The piston cycle is monitored with an optical sensor on the engine shaft. The 11 mm long nylon duct that separates engine from cold heat exchanger (HXF) serves as a mount for a pressure transducer as well as a thermal break between the warm engine and HXF. The Si wafer stack length and wafer arrangement can be varied (although not in these tests). The room temperature heat exchanger (HXL) on the back of the stack separates the stack from the horncone section. A pressure transducer is mounted just behind HXL. These two pressure locations allow for estimation of the average pressure fluctuation level in the stack, as well as phase relative to the piston. The horncone was designed in 3 segments to allow variation of the internal volume and thereby allow varying the pressure fluctuation amplitude ($|p|/Pm$). Using only the first segment of the horncone results in $|p|/Pm \cong 8\%$, adding the second segment reduces $|p|/Pm \cong 6\%$, and adding the third segment reduces $|p|/Pm \cong 3\%$. The horncone design allows a large change in volume with a minimum change in length to maintain a high resonant frequency.

The resonant frequency is always above 600 Hz, which ensures that the device runs

below resonance. The pressure and velocity distributions for the intermediate length case (|p|/Pm ≅ 6%) are as shown in Fig. 5, which also results in the cold end of the stack oriented toward the engine. At low frequency (50 Hz, Fig. 5) the pressure fluctuation amplitude is uniform thoughout the device, simple compression and expansion. At 300 Hz the pressure fluctuation levels are seen to drop some at the piston; at resonance the piston would become a pressure node. Fig. 5 also shows the volume velocity which drops from a maximum at the piston face to zero at the back of the horncone. Thus the pressure fluctuation levels across the stack are approximately level, moreso for lower frequencies and shorter device length, and the velocity fluctuation amplitude (and displacement amplitude) decrease steadily from HXF toward HXL, with the rate of decrease depending on the device length. Thus the "short stack" approximation is not valid but this poses no problem for comparison of different stacks of the same length.

Concluding Remarks

The mTAP device design has been presented - new small-scale thermoacoustics refrigerator *stack* using micro-machined technique. The unique approach is to use several MEMS fabricated silicon wafers with equally spaced gap as the stack. Current results show that this concept seems promising to future application. Further work is underway to study its thermoacoustic characteristics.

Acknowledgement

The author gratefully thanks the NSC for providing funding for this project.

References

Adeff, J.A., Hofler, T.J., Atchley, A.A, "Measurements with reticulated vitreous carbon (RVC) stacks in thermoacoustic prime movers and refrigerators," JASA V104 (1), p32, July 1998.

Adeff, J.A., and Hofler, T.J., 2000, "Design and construction of a solar-powered, thermo-acoustically driven, thermoacoustic refrigerator," presented at ASA Atlanta meeting, June 2000, and available online at: http://www.physics.nps.navy.mil/hofler/stadtar.htm

Bosel, J., Trepp, C., Fourie, J.G., "An alternative stack arrangement for thermoacoustic pumps and refrigerators," JASA V106 (2), p707, August 1999.

Holmberg, D.G., Chen, G.H., Wo, A.M., and Lin, H.T., "Thermal modeling and performance analysis of a thermoacoustic refrigerator," submitted to JASA, in review.

Incropera, F.P., and DeWitt, D.P., 1985, Fundamentals of Heat and Mass Transfer, John Wiley and Sons, New York, 2nd ed.

Swift, G.W., 1988, "Thermoacoustic engines," J. Acoust. Soc. Am. 84 (4).

Swift, G.W., 1999, "Thermoacoustics: a unifying perspective for some engines and refrigerators", Los Alamos Nat'l Lab, Fourth Draft, Autumn 1999, LA-UR 99-895, available online at http://www.lanl.gov/projects/thermoacoustics/

Ward, B., and Swift, G.W., 1996, "Design Environment for Low-amplitude Thermoacoustic Engines," Los Alamos National Laboratory, LA-CC-93-8.

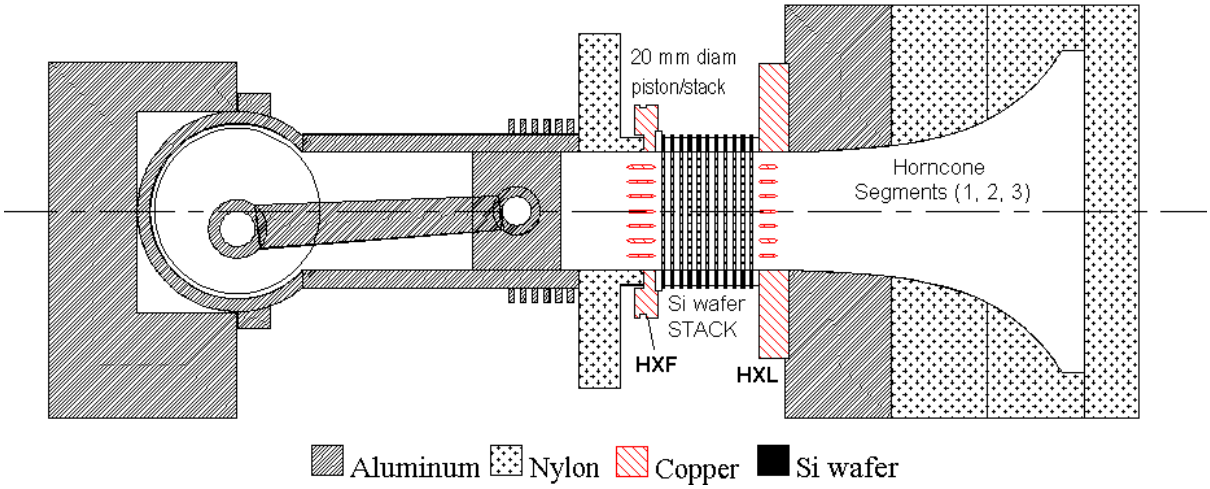

Fig. 1 Micro thermoacoustic test platform (mTAP) schematic (to scale).

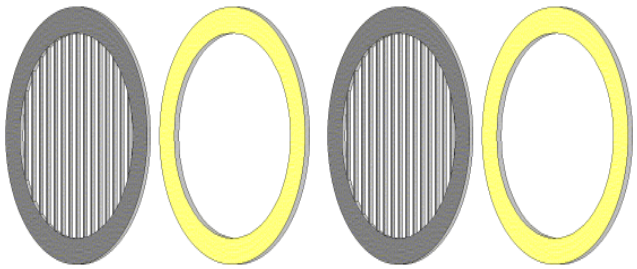

Fig. 2 Si stacked-wafer stack schematic showing etched Si wafers and spacer rings.

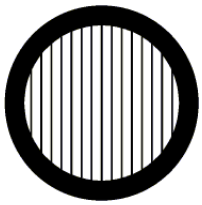

Fig. 3 Si wafer showing etched parallel plate structure, filament width 0.2mm, spacing between 1.1 mm, inside diameter 20 mm.

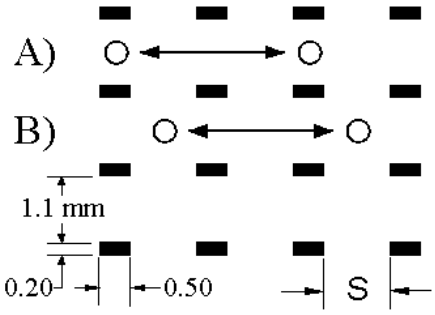

Fig. 4 Stack viewed from side showing cross-section of 0.2 mm x 0.5mm filaments and 1.1 mm filament spacing and axial spacing **S** between wafers with two oscillating air parcels represented by circles. At the end points of its cycle, particle (A) must exchange energy with the filament above or below, while particle (B) must be within close enough proximity with filaments upstream and downstream to exchange energy.

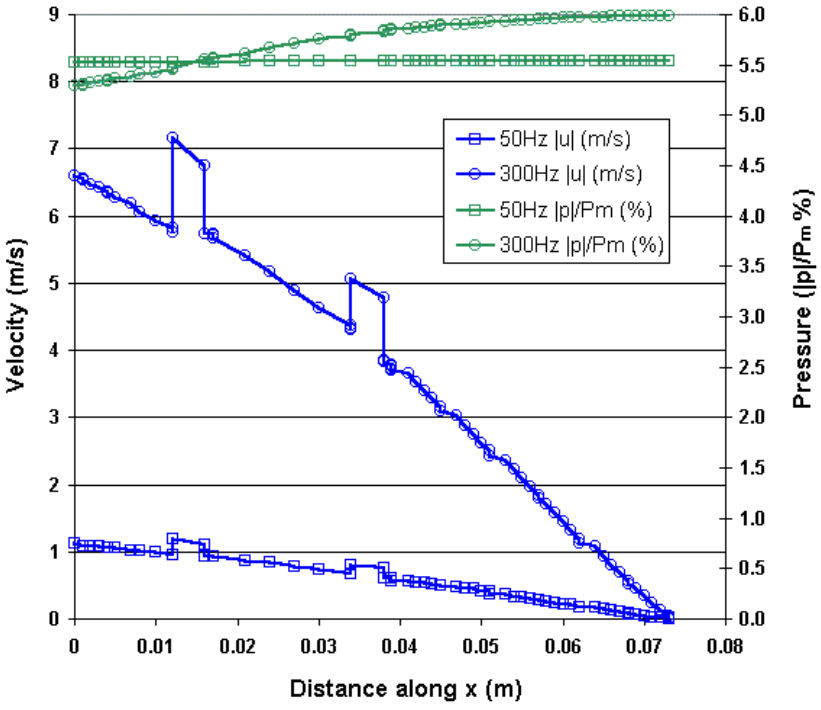

Fig. 5 DeltaE predicted pressure fluctuation level (right axis) and velocity fluctuation levels along length of mTAP device at 50 Hz and 300 Hz for the middle length (segment 2 of horncone) configuration.